HHS Public Access

Author manuscript

Nature. Author manuscript; available in PMC 2013 July 31.

Published in final edited form as:

Nature. 2013 January 31; 493(7434): 684–688. doi:10.1038/nature11738.

Visualization of splenic marginal zone B cell shuttling and follicular B cell egress

Tal I. Arnon, **Robert M. Horton**, **Irina L. Grigorova**, and **Jason G. Cyster**

Howard Hughes Medical Institute and Deparmtnet of Microbiology and Immunology, University of Califrnia, San Francisco, CA, 94143

Abstract

The splenic marginal zone (MZ) is a unique microenvironment where resident immune cells are exposed to the open blood circulation[1,2]. Despite its importance in responses against blood-borne antigens, lymphocyte migration in the MZ has not been intravitally visualized due to challenges associated with achieving adequate imaging depth in this abdominal organ. Here we develop a 2-photon microscopy procedure to study MZ and follicular (FO) B cell movement in the live spleen. We show that MZ B cells are highly motile and exhibit long membrane extensions. MZ B cells shuttle between MZ and follicles with at least one fifth of the cells exchanging between compartments per hour, a behavior that explains their ability to rapidly deliver antigens from the open blood circulation to the secluded follicles. FO B cells also transit from follicles to MZ but unlike MZ B cells, they fail to undergo integrin-mediated adhesion, become caught in fluid flow and are carried into the red pulp. FO B cell egress via the MZ is sphingosine-1-phosphate receptor-1 (S1PR1)-dependent. This study shows that MZ B cells migrate continually between MZ and follicles and establishes the MZ as a site of S1PR1-dependent B cell exit from follicles. The work also shows how adhesive differences of closely related cells critically influences their behavior in the same microenvironment.

MZ B cells are a unique B cell subset that plays a pivotal role in mounting antibody responses against systemic pathogens[3,4]. Early studies of MZ B cells in rodents showed that they are non-recirculating and are restricted to the spleen[5]. MZ B cells were later found to have elevated integrin expression and to depend on integrins to be retained in the MZ[6]. These observations gave the impression that the cells were poorly motile. Yet MZ B cells mediate the delivery of opsonized antigens from MZ to FOs[7–9] and recent studies provided indirect evidence that MZ B cells continually exchange between MZ and FO[9,10]. However, this cellular behavior has not been directly visualized and its existence is not fully accepted. To permit real-time imaging of MZ B cells we developed an approach to label these cells. We noted evidence that FO B cells can give rise to MZ B cells[4,11,12] and that MZ B cells, but not FO B cells, are self-renewing in the absence of input from less committed

Address correspondence to Jason G. Cyster: Jason.Cyster@ucsf.edu: Phone (415) 502-6427; Fax (415) 502-8424.

Author contributions

TIA and JGC conceived and designed the experiments. TIA performed the experiments. RMH helped with some of the quantitative image analysis. ILG helped with early aspects of the spleen surgery procedure. TIA and JGC wrote the manuscript.

precursors[13]. We therefore asked whether FO B cells could selectively reconstitute the MZ of CD19-deficient mice that have an empty MZ B cell niche, but a normal FO compartment[12,14,15]. When GFP$^+$ B cells were transferred into CD19 KO mice and analyzed after 8 weeks, there was substantial reconstitution of the MZ B cell compartment (Fig. 1a). Moreover, typically ~90% of the transferred GFP$^+$ cells had a MZ B cell phenotype (Fig. 1b and Suppl. Fig. S1). Like their normal counterparts[16], the reconstituted MZ B cells were poised to respond to antigen and LPS (Suppl. Fig. S1). To determine if the reconstituted MZ B cells were positioned correctly we labeled blood-exposed cells by i.v. injection of a fluorescently conjugated antibody 5 min prior to tissue isolation[9,10]. This analysis, as well as immunofluoresence microscopy, indicated that 50–60% of the MZ B cells were in the MZ whereas the remaining cells were located in the FOs (Fig. 1c, d), similar to their distribution in WT mice[9,10]. Moreover, the reconstituted mice showed a rescued ability to deposit an opsonized antigen on follicular dendritic cells (FDCs) over a 16 hour period (Fig. 1e and Suppl. Fig. S1). Consistent with a direct role of the MZ B cells in the delivery of opsonized antigen to FDCs, reconstitution with CR2$^{-/-}$ MZ B cells failed to restore antigen delivery (Suppl. Fig. S1).

For intravital two-photon laser scanning microscopy (TPLSM), CD19 KO mice reconstituted with ~1:2 mixtures of GFP$^+$ and non-labeled B cells were injected with phycoerythrin-immune complexes (PE-ICs) two hours before imaging. Tissue section analysis established that PE-ICs were concentrated on SIGN-R1$^+$ MZ macrophages in the first hours after injection, providing a means for locating this compartment (Fig. 2a). The spleen was surgically exposed, bathed in saline and stabilized by attachment to a platform placed over the mouse abdomen. Typically one or two white pulp cords per spleen passed sufficiently near the capsule to permit visualization (Suppl. Fig. S2). MZ B cells were identified as being situated in the MZ or FO based on whether their location overlapped with or was internal to the ring of PE-IC labeled macrophages (Fig. 2b, c). Contours were drawn immediately internal to the PE-IC labeled cells in each z-plane and used to generate a three dimensional surface (Fig. 2b) that approximated the position of the marginal sinus separating MZ and FOs[1,2].

MZ B cells within both the MZ and FO were migratory (Fig. 2c,d and Movies S1 and S2). They traveled with similar velocities in both compartments, but cells within the MZ showed sharper turning angles and less straightness in their migration paths (Fig. 2d) indicating a greater amount of confinement. MZ B cells were larger than FO B cells, as expected[16], and they exhibited a probing, dendritic morphology (Fig. 2e and Movies S1–S2) reminiscent of that seen for GC B cells[17]. In some cases (~20%) the MZ B cells exhibited trailing processes of remarkable length, occasionally exceeding 40μm (Fig. 2c,e and Movie S2). Similar morphologies were observed for cells located in the MZ and FO.

Treatment with FTY720 to disrupt S1PR1 function causes MZ B cells to leave the MZ and locate within the FO[18]. Analysis of this repositioning at four time points using CD19-PE labeling of blood-exposed spleen cells suggested that it was complete within 30 min (Fig. 2f and Suppl. Fig. S3). A similar rate of MZ B cell relocation was observed by TPLSM (Fig. 2g, Suppl. Fig. S3 and Suppl. Movie 3) indicating that the behavior remained intact during the intravital imaging procedure.

To examine the rate of MZ B cell movement between MZ and FO in untreated mice, the tracks of cells that crossed between zones were manually annotated and counted (Fig. 3). MZ B cells moving from the MZ across the boundary into the FO were readily observed (Fig. 3a and Movie S4). MZ B cells could also be seen migrating from the FO to the MZ (Fig. 3b and Movies S5). Similar observations were made when the boundary between FO and MZ was defined using transferred FO B cells rather than by PE-IC labeling (Suppl. Fig. S4) indicating that the migratory behavior of MZ B cells was not a consequence of exogenous IC exposure. This analysis showed that at least 10% of the MZ cells that were tracked during a 30 minute imaging session moved from MZ to FO, and a similar fraction of the MZ cells that started in the FO moved to the MZ (Fig. 3c). On some occasions during passage across the boundary the MZ B cells paused (Movies S4, example 1 and S5) and sometimes they moved parallel to the surface before crossing (Movie S4, example 2). During the crossing event, some cells showed an obvious constriction of the cell body (Fig. 3a, Suppl. Fig. S4b lower, and Movie S4, example 2). We also observed several cells that remained tethered near the MZ–FO interface by a membrane process while the cell body moved back and forth between zones (Movie S2, yellow dashed circle).

As a separate approach to estimate the rate of MZ B cell movement from FOs to MZ, in this case at the level of the whole spleen, we took advantage of the essential role of integrins in mediating MZ B cell retention in the MZ. Treatment with integrin-blocking antibodies causes selective loss of cells from the MZ while not displacing cells that are situated within FOs[6]. Using this approach, loss of MZ B cells from FOs would occur over time as cells move from the FO into the MZ. Mice were treated with integrin-neutralizing antibodies and the rate of MZ B cell decay from FOs was determined by enumerating the *in vivo* CD19-PE unlabeled MZ B cells remaining in the spleen over time. The decay rate matched first order kinetics with a t1/2 of ~2.5 hrs (Fig. 3d) consistent with the estimate from TPLSM of 20% exchange between FO and MZ per hour.

An exchange rate of 20% per hour indicates that some MZ B cells remain within the MZ for several hours. S1PR1 is required for MZ B cells to remain in the MZ[18] and when it is down-modulated the cells relocalize into the FO within ~30 min (Fig. 2f, g). The level of S1PR1 on MZ B cells in the spleen was higher than on MZ B cells that had been transferred into blood for one hour (Fig. 3e) and was more similar to cells exposed *in vitro* to low nM S1P concentrations (Suppl. Fig. S5). RBCs, the main source of blood S1P, were detectable in the MZ but were sparse compared to their density in blood vessels and in the red pulp (Suppl. Fig. S5). A lower interstitial S1P concentration may cause a more gradual or less complete S1PR1 down-modulation than occurs on cells in circulatory blood, allowing for a several hour dwell time in the MZ.

We next examined the migration dynamics of FO B cells. Intravital TPLSM of the spleen a day after intravenous transfer of FO B cells showed a marked concentration of the cells within FOs (Fig. 4a). The FO B cells migrated with a similar speed to MZ B cells and the two types of cell showed similar displacement over time while migrating within the FO (Fig. 4b). As well as cells confined to FOs, transferred B cells could be visualized in the adjacent red pulp (Fig. 4c). In many cases the cells appeared to be moving in a tangent away from the FO (Fig. 4c). B cells within the red pulp had a more rounded morphology than cells within

the FO and their axis ratio was ~30% reduced (Fig. 4d). In contrast to the active migratory behavior of B cells within the FO, many B cells within the red pulp failed to show evidence of active migration but were instead intermittently stationary and fast moving (Fig. 4e and Movie S6). Occasionally during a fast moving step the cell would disappear from view, possibly indicating it had passed into a red pulp venule to be flushed from the spleen (Movie S6). Manual tracking of 550 red pulp B cells showed that while many were stationary during the imaging period, 3-fold more cells appeared to move passively (fast and tangentially) versus actively (slow and meandering) (Fig. 4f).

The pathway by which FO B cells exit from splenic FOs is not defined. One possible route these cells might take is by crossing the MZ sinuses, similarly to MZ B cells. In agreement with this hypothesis, tracking FO B cell migration with respect to the surface generated using PE-IC labeled MZ macrophages, allowed the identification of cells migrating into the MZ (Fig. 4c, g and Suppl. Fig. S6a). Frequently, upon entering this region the FO B cells underwent a jump in movement, perhaps a consequence of being caught in a region of flow (Fig. 4g, Suppl. Figure 6a and Movies S7). The cells were usually retained moments later; some cells then appeared non-migratory during the rest of the imaging session (Movie S7, example 1) while others did continue to move (Movie S7, example 3). Axis ratio measurements of cells that crossed between zones showed that WT FO B cells promptly became rounded after crossing into the MZ (Fig. 4h).

To test whether the striking difference in MZ and FO B cell behavior within the MZ was a consequence of integrin-mediated adhesion, we examined the behavior of GFP^+ MZ B cells in reconstituted CD19 KO mice in the first hours after treatment with integrin neutralizing antibodies. Under these conditions, MZ B cells in the MZ frequently ceased active migration, became rounded and then moved fast and tangentially in the direction of the red pulp (Fig. 4i–l, Suppl. Fig. S6 and Suppl. Movies S8). This change in behavior was associated with a sharp increase in displacement over time (Fig. 4k, l). By contrast, MZ B cells within the FO continued to migrate and they maintained their long membrane extensions (Fig. 4I and Suppl. Fig. S6), though their displacement over time was slightly reduced (Fig. 4l and not shown) as observed for integrin-deficient cells in lymph nodes[19,20].

Although S1PR1 and S1P have been argued to play a role in lymphocyte egress from the spleen[21] this conclusion has been based on indirect assessments and it has also been suggested that the spleen is distinct from other lymphoid organs in not being sensitive to egress inhibition by FTY720[22,23]. This lack of clarity arises in part because cell entry to and exit from the spleen both occur via the blood and because the S1PR1-dependent egress step has not been visualized. To test whether S1PR1 was required for FO B cell movement from FO to MZ, we cotransferred fluorescently labeled WT and S1PR1-deficient B cells into wild-type recipients and performed TPLSM (Fig. 4m). Plotting the tracks of all FO B cells for a 30 min imaging session led to filling of the follicular area and the high density region of tracks was used to generate a marginal sinus-approximating surface (Fig. 4m and Suppl. Fig. S7). S1PR1-deficient B cells moved within the FO with similar velocities and turning angles to WT B cells (Movie S9 and data not shown). However, very few S1PR1-deficient B cells were observed exiting from FOs into the MZ (Fig. 4m, n and Movie S9). In the rare cases where such movement was scored, no examples of cells undergoing the jump in

movement were seen (Movie S9). A summary of these experiments showed that at least 10-fold fewer S1PR1-deficient than WT B cells crossed out of the white pulp per hour (Fig. 4n).

The perpetual oscillatory movement of MZ B cells observed here represents possibly the fastest rate of cellular exchange between tissue compartments so far defined and provides a mechanism for rapid delivery of opsonized blood-borne antigens into splenic FOs: MZ B cells capture antigens via complement receptors while travelling through the MZ and then pass them off to FDCs while migrating in the FOs. Remarkably, MZ B cells exhibit similar dynamics while resisting shear and migrating in an integrin-dependent fashion in the MZ and when moving in a largely integrin-independent fashion in the FO. Precedent for a single cell type migrating with similar characteristics in an integrin-dependent and -independent manner is provided by findings in an in vitro system with dendritic cells[24]. The factors promoting formation of the long trailing processes exhibited by many MZ B cells are unclear but these membrane extensions may facilitate interactions with NKT cells[25] or with FO B cells scanning for surface displayed antigens[26]. FO B cells have lower integrin-adhesive activity than MZ B cells[6] and our data indicate that upon passage into the MZ they are unable to activate sufficient integrin activity to resist the local shear forces of blood flow and they become rounded and travel passively into the red pulp. As well as defining an S1PR1-dependent pathway of B cell egress from the spleen, these results highlight how adhesive differences of closely related cells critically influences their behavior in the same microenvironment.

Methods Summary

Adoptive transfer, selective reconstitution of MZ B cells and intravital imaging of the spleen

B cells from Ub-GFP^{+} (4×10^6) or non-tg (8×10^6) mice were co-transferred to CD19$^{-/-}$ recipient mice for 8–12 wks. For imaging FO B cells, purified B cells (~40×10^6) from B6 or S1P1$^{fl/-}$Mb1Cre/+ mice were labeled with fluorescent dye and transferred 24 hrs before imaging. To label MZ macrophages, mice were injected with PE-ICs 2hrs before imaging. All imaging experiments were done intravitally using two-photon laser scanning microscopy. To prepare for imaging, mice were anesthetized[17], a skin incision was made bellow the costal margin and the spleen was gently exposed on its stalk. To immobilize the spleen, a spring-loaded platform [38] was placed over the mouse and screwed down. Saline was added to the contact area between the spleen and the cover slip. Tracks generated using Imaris Bitplane software were manually examined and verified.

Supplementary Material

Refer to Web version on PubMed Central for supplementary material.

Acknowledgments

We thank Mark Miller for help with the microscope stage mount, Tri Phan for helpful advice regarding mouse surgery, Jinping An for excellent technical assistance and Oliver M Bannard, Jagan R Muppidi, Michael Barnes and Andrea Reboldi for comments on the manuscript. T.I.A. was supported by a Jane Coffin Child's fellowship and

J.G.C. is an Investigator of the Howard Hughes Medical Institute. This work was supported in part by NIH grant AI74847.

References

1. Schmidt EE, MacDonald IC, Groom AC. Comparative aspects of splenic microcirculatory pathways in mammals: the region bordering the white pulp. Scanning Microsc. 1993; 7:613–628. [PubMed: 8108677]
2. Mebius RE, Kraal G. Structure and function of the spleen. Nat Rev Immunol. 2005; 5:606–616. [PubMed: 16056254]
3. Martin F, Kearney JF. Marginal-zone B cells. Nat Rev Immunol. 2002; 2:323–335. [PubMed: 12033738]
4. Pillai S, Cariappa A. The follicular versus marginal zone B lymphocyte cell fate decision. Nature Reviews Immunology. 2009; 9:767–777.
5. MacLennan ICM, Gray D, Kumararatne DS, Bazin H. The lymphocytes of splenic marginal zones: a distinct B-cell lineage. Immunol Today. 1982; 3:305–307. [PubMed: 25290472]
6. Lu TT, Cyster JG. Integrin-mediated long-term B cell retention in the splenic marginal zone. Science. 2002; 297:409–412. [PubMed: 12130787]
7. Guinamard R, Okigaki M, Schlessinger J, Ravetch JV. Absence of marginal zone B cells in Pyk-2 deficient mice define their role in the humoral response. Nat Immunol. 2000; 1:31–36. [PubMed: 10881171]
8. Ferguson AR, Youd ME, Corley RB. Marginal zone B cells transport and deposit IgM-containing immune complexes onto follicular dendritic cells. Int Immunol. 2004; 16:1411–1422. [PubMed: 15326094]
9. Cinamon G, Zachariah M, Lam O, Cyster JG. Follicular shuttling of marginal zone B cells facilitates antigen transport. Nat Immunol. 2008; 9:54–62. [PubMed: 18037889]
10. Arnon TI, Xu Y, Lo C, Pham T, An J, Coughlin S, Dorn GW, Cyster JG. GRK2-dependent S1PR1 desensitization is required for lymphocytes to overcome their attraction to blood. Science. 2011; 333:1898–1903. [PubMed: 21960637]
11. Kumararatne DS, MacLennan IC. Cells of the marginal zone of the spleen are lymphocytes derived from recirculating precursors. Eur J Immunol. 1981; 11:865–869. [PubMed: 6976895]
12. You Y, Zhao H, Wang Y, Carter RH. Cutting edge: Primary and secondary effects of CD19 deficiency on cells of the marginal zone. J Immunol. 2009; 182:7343–7347. [PubMed: 19494255]
13. Hao Z, Rajewsky K. Homeostasis of peripheral B cells in the absence of B cell influx from the bone marrow. J Exp Med. 2001; 194:1151–1164. [PubMed: 11602643]
14. Makowska A, Faizunnessa NN, Anderson P, Midtvedt T, Cardell S. CD1high B cells: a population of mixed origin. Eur J Immunol. 1999; 29:3285–3294. [PubMed: 10540340]
15. Martin F, Kearney JF. Positive selection from newly formed to marginal zone B cells depends on the rate of clonal production, CD19, and btk. Immunity. 2000; 12:39–49. [PubMed: 10661404]
16. Oliver AM, Martin F, Gartland GL, Carter RH, Kearney JF. Marginal zone B cells exhibit unique activation, proliferative and immunoglobulin secretory responses. Eur J Immunol. 1997; 27:2366–2374. [PubMed: 9341782]
17. Allen CD, Okada T, Tang HL, Cyster JG. Imaging of germinal center selection events during affinity maturation. Science. 2007; 315:528–531. [PubMed: 17185562]
18. Cinamon G, Matloubian M, Lesneski MJ, Xu Y, Low C, Lu T, Proia RL, Cyster JG. Sphingosine 1-phosphate receptor 1 promotes B cell localization in the splenic marginal zone. Nat Immunol. 2004; 5:713–720. [PubMed: 15184895]
19. Woolf E, Grigorova I, Sagiv A, Grabovsky V, Feigelson SW, Shulman Z, Hartmann T, Sixt M, Cyster JG, Alon R. Lymph node chemokines promote sustained T lymphocyte motility without triggering stable integrin adhesiveness in the absence of shear forces. Nat Immunol. 2007; 8:1076–1085. [PubMed: 17721537]
20. Boscacci RT, Pfeiffer F, Gollmer K, Sevilla AI, Martin AM, Soriano SF, Natale D, Henrickson S, von Andrian UH, Fukui Y, Mellado M, Deutsch U, Engelhardt B, Stein JV. Comprehensive analysis of lymph node stroma-expressed Ig superfamily members reveals redundant and

nonredundant roles for ICAM-1, ICAM-2, and VCAM-1 in lymphocyte homing. Blood. 2010; 116:915–925. [PubMed: 20395417]

21. Schwab SR, Cyster JG. Finding a way out: lymphocyte egress from lymphoid organs. Nat Immunol. 2007; 8:1295–1301. [PubMed: 18026082]
22. Rosen H, Sanna MG, Cahalan SM, Gonzalez-Cabrera PJ. Tipping the gatekeeper: S1P regulation of endothelial barrier function. Trends Immunol. 2007; 28:102–107. [PubMed: 17276731]
23. Morris MA, Gibb DR, Picard F, Brinkmann V, Straume M, Ley K. Transient T cell accumulation in lymph nodes and sustained lymphopenia in mice treated with FTY720. Eur J Immunol. 2005; 35:3570–3580. [PubMed: 16285007]
24. Schumann K, Lammermann T, Bruckner M, Legler DF, Polleux J, Spatz JP, Schuler G, Forster R, Lutz MB, Sorokin L, Sixt M. Immobilized chemokine fields and soluble chemokine gradients cooperatively shape migration patterns of dendritic cells. Immunity. 2010; 32:703–713. [PubMed: 20471289]
25. Barral P, Sanchez-Nino MD, van Rooijen N, Cerundolo V, Batista FD. The location of splenic NKT cells favours their rapid activation by blood-borne antigen. EMBO J. 2012; 31:2378–2390. [PubMed: 22505026]
26. Suzuki K, Grigorova I, Phan TG, Kelly L, Cyster JG. Visualizing B cell capture of cognate antigen from follicular dendritic cells. J Exp Med. 2009; 206:1485–1493. [PubMed: 19506051]

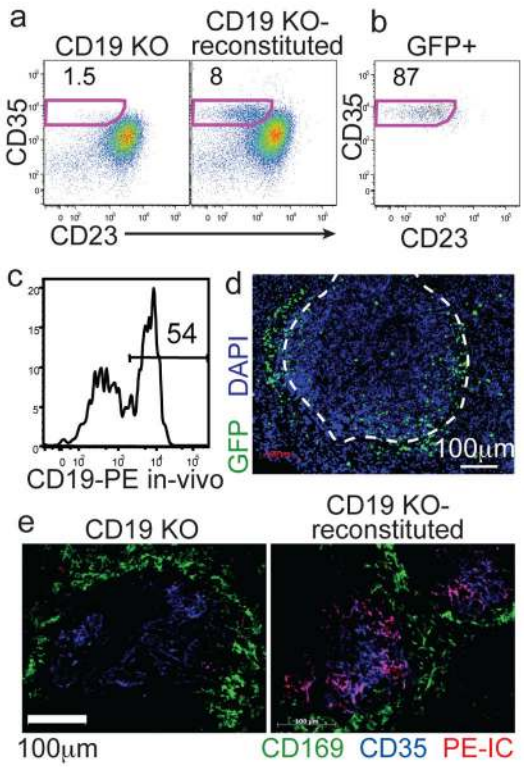

Figure 1. Adoptive transfer system for GFP labeling MZ B cells

(**a**) Frequency of CD35hiCD23lo MZ B cells amongst B220+ cells in CD19−/− mice before (left) or 8 wks after (right) transfer of GFP+ B cells. (**b**) Phenotype of CD19+ GFP+ B cells from A. Numbers indicate % of cells in gate. (c) In vivo anti-CD19PE labeling of MZ-phenotype (CD23loCD35hi) B cells. (**d**) Spleen section from mouse reconstituted with 2:1 mixture of non-tg and GFP+ B cells, stained with anti-GFP (green) and DAPI (blue). Marginal sinus is indicated by the dashed white line. (**e**) Spleen sections from the indicated mice that had received PE-IC (red) 16hr earlier, stained for CD169 (green) and CD35 (blue).

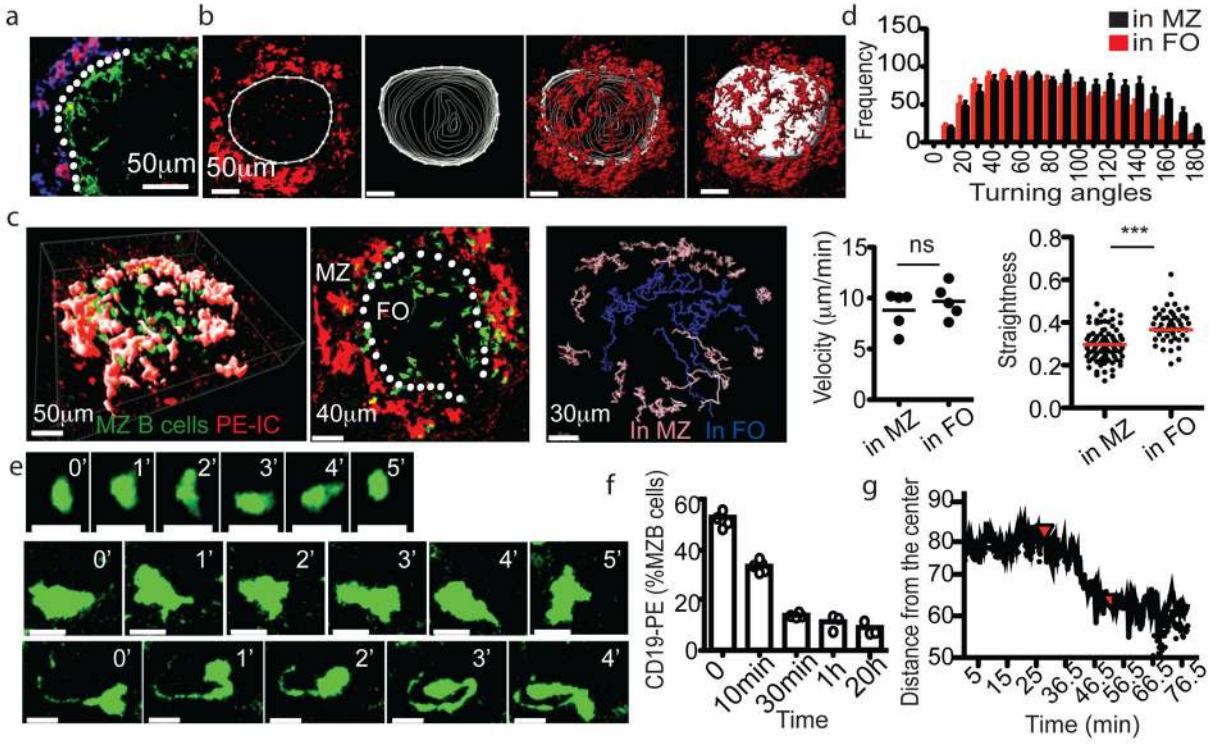

Figure 2. MZ B cells are migratory and exhibit long membrane processes

(**a**) Figure 4. Splenic FO B cell migration and S1PR1 requirement for exit a) Spleen section showing PE-IC (red), SIGN-R1 (blue) and CD169 (green) distribution two hours after PE-IC injection. White dotted line indicates location of sinus. (**b**) Generation of MZ-FO boundary surface. Left image shows an example contour drawn ~10μm internal to the PE-ICs to represent the boundary in a single x–y slice (3μm). Middle images show contours drawn for each slice in the 60μm z stack. Right image shows final surface with overlaid PE-IC stain. (**c**) TPLSM of GFP+ MZ B cells in reconstituted CD19−/− spleen. Left panel shows a 57μm z-projection view. Middle panel shows a 30μm slice from the center of this region. Location of marginal sinus is indicated (white dotted line). Right, representative classification of MZ B cell tracks based on positioning with respect to surface. Pink, in MZ; blue, in FO. (**d**) Median velocity, distribution of turning angles and straightness of MZ B cells (5 data sets from 3 mice). (**e**) Time-lapse images of two MZ B cells (middle and bottom panels) compared with a FO B cell (top panels). All cells are GFP+. Scale bars, 10μm. (**f, g**) Kinetics of MZ B cell displacement into the FO following FTY720 treatment. (**f**) Frequency of in vivo anti-CD19-PE labeled MZ B cells at the indicated time after FTY720 injection (n=6 mice), detected by flow cytometry. (**g**) Average distance of GFP+ MZ B cells from the most center point over time during TPLSM imaging. Red arrow at 25 min, time of FTY720 injection. (Second red arrow, time of anesthetic reinjection). In d, c, f, bars or lines indicate means (error bars, SEM). *** $p<0.0005$ and ns, not significant ($p>0.05$) by unpaired Student's t-test.

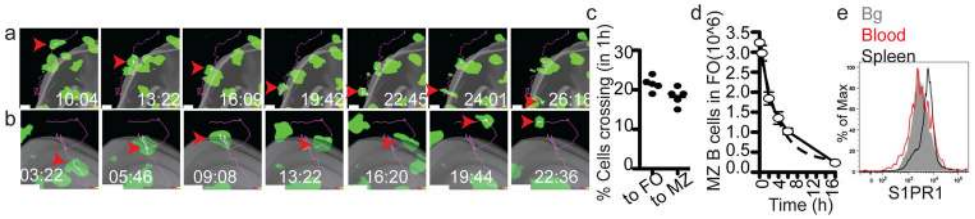

Figure 3. MZ B cells migrate bidirectionally between MZ and FO

(**a**) MZ B cell crossing from MZ into FO. (**b**) MZ B cell migrating from FO to MZ. Grey surface represents MZ-FO interface. Time lapse is in min:sec. Arrowheads point to cell location at each time point and line indicates tracked path of cell. (**c**) MZ B cells shuttling rate (5 data sets from 3 mice). (**d**) Decay rate of MZ B cells from the FO following integrin blockade. The number of MZ B cells remaining in the FO was determined at each time point, showing a decay rate of 23% per hour (1 representative experiment out of 3). (**e**) Flow cytometric analysis of S1PR1 on MZ B cells in spleen (blue line) or after 1hr exposure to blood (red line). Bg, background.

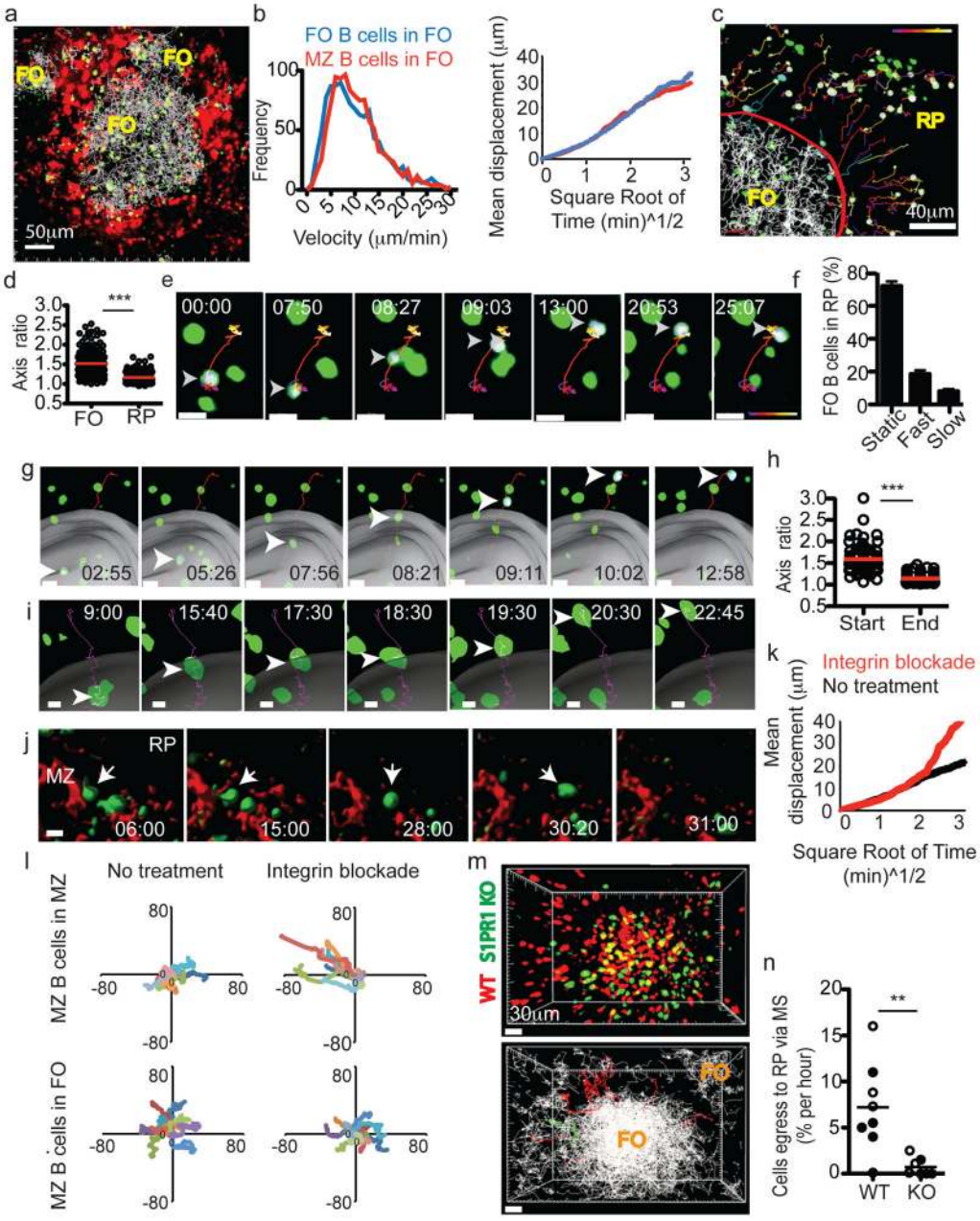

Figure 4. Splenic FO B cell migration and S1PR1 requirement for exit

(**a**) 54μm z-projection view showing transferred FO B cells (green) and their tracks (white lines) and PE-IC-labeled macrophages (red). (**b**) Instantaneous velocities (left) and displacement versus square root of time (right) of FO and MZ B cells in the FO. Data from at 5–6 experiments (3–4 mice). (**c**) 45μm z-projection view of FO B cells (green) in FO and red pulp (RP). Red line, MZ-FO border; white lines, tracks of FO B cells in FO; time-coded colored lines, FO B cells in RP; blue lines, FO B cells in transition from FO to MZ. Cells tracked outside the FO are highlighted with a white surface. (**d**) Axis ratio of FO B cells in FO and RP. (**e**) FO B cell movement in the RP. (**f**) Percentage of cells in RP exhibiting stationary (‘Static’), rapid (‘Fast’) or migratory (‘Slow’) behavior (5 experiments in 3 mice,

n= 550 cells). (**g**) FO B cell crossing from FO to MZ. Grey surface, MZ–FO interface. (**h**) Axis ratio of FO B cells migrating from FO to MZ at start and end of track (n= 24 cells). (**i–l**) Intravital TPLSM of MZ B cells following integrin blockade. (i) MZ B cell crossing from FO to MZ. (**j**) MZ B cell movement from MZ to RP. (**k**) Displacement versus square root of time (right) of MZ B cells in the MZ before (black) and two hours after (red) integrin blockade. (**l**) Superimposed 10-min tracks of randomly selected MZ B cells, in the x–y plane. Units are in micrometers. Data for I–L were from 8 experiments (3 mice). (**m**) Upper, 90μm z-projection view of WT (red) and S1PR1 KO (green) FO B cells in spleen. Lower, automated tracks of transferred B cells (white). Tracks of WT cells (11 red lines) and KO cells (1 green line) leaving FO are shown. (**n**) FO egress rate of WT and S1PR1 KO B cells. Open circles, MZ–FO interface determined based on PE-IC labeling; filled circles, interface determined based on FO B cell tracks. In e, g, I, j, elapsed time is in min:sec, arrowheads point to tracked cells and scale bar indicates 10μm. In f, h, n, bars or lines represent mean (error bars in f, ±SEM).